Supporting information

PtZn vs. PtGa in CO_2 Hydrogenation: When Alloy Stability and Redox Dynamic Drives Selectivity

Wei Zhou[1], C. S. Praveen[2], Wei Wang[1], Chenxi He[3], Takashi Toyao[3], Ken-ichi Shimizu[3], Ryo Toyoshima[4], Hiroshi Kondoh[5], Yuhao Wang[6], Chunliang Wang[6], James Paterson[7], Jamie Southouse[7], Carlo Federico Pauletti[8], Aleix Comas Vives[8,9†] and Christophe Copéret[1]*

[1]*Department of Chemistry and Applied Biosciences, ETH Zürich, CH-8093 Zurich*

[2]*International School of Photonics, Cochin University of Science and Technology, Cochin, Kerala, 682022*

[3]*Institute for Catalysis, Hokkaido University, Sapporo 001-0021*

[4]*Department of Materials Engineering, The University of Tokyo, Tokyo 113-0033*

[5]*Department of Chemistry, Keio University, Yokohama 223-8522*

[6]*Engineering Research Center of Metallurgical Energy Conservation and Emission Reduction, Ministry of Education, Kunming University of Science and Technology, Kunming 650093*

[7]*Applied Science and Technology, bp Technology, bp plc, Saltend, Hull, HU12 8DS*

[8]*Institute of Materials Chemistry, Technische Universität Wien, Vienna 1060*

[9]*Departament de Química, Universitat Autònoma deBarcelona, Cerdanyola del Vallès 08193 Catalonia*

[†]Present address: *Institute of Materials Chemistry, Technische Universität Wien, Vienna 1060*

*Corresponding author: ccoperet@ethz.ch

Supporting figures and tables

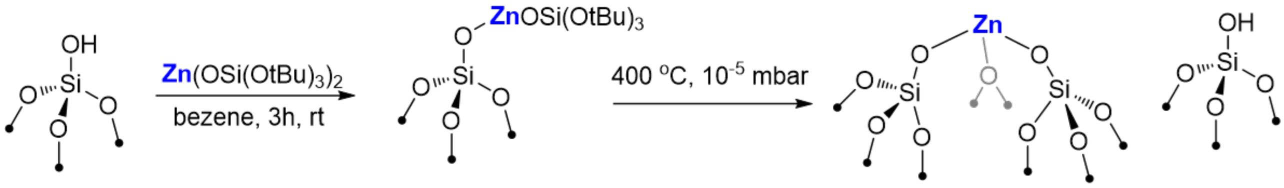

Figure S1. Schematic procedure for the synthesis of $Zn^{II}@SiO_2$.

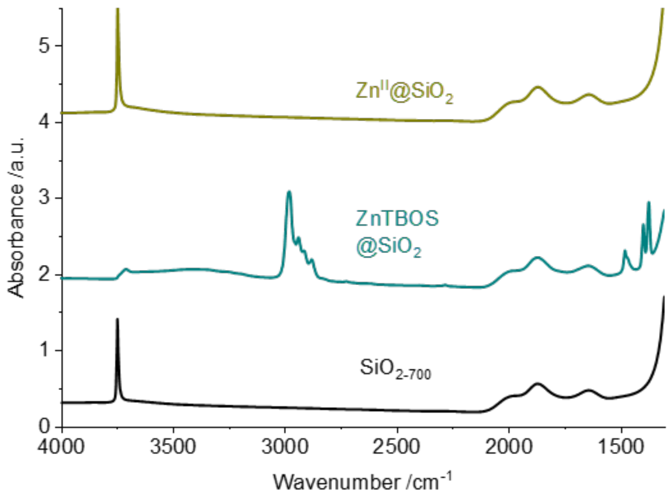

Figure S2. IR spectra throughout the synthesis of Zn^{II}@SiO_2.

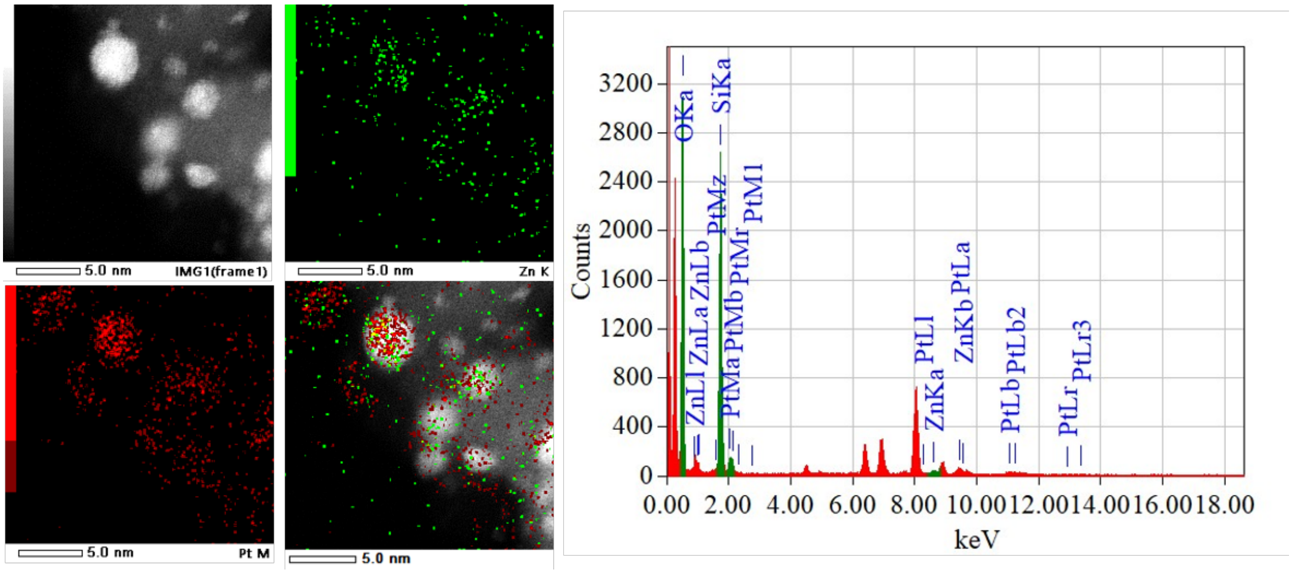

Figure S3. STEM EDX analysis of PtZn@SiO_2. EDX Maps (left) of the investigated area and EDX-spectrum (right).

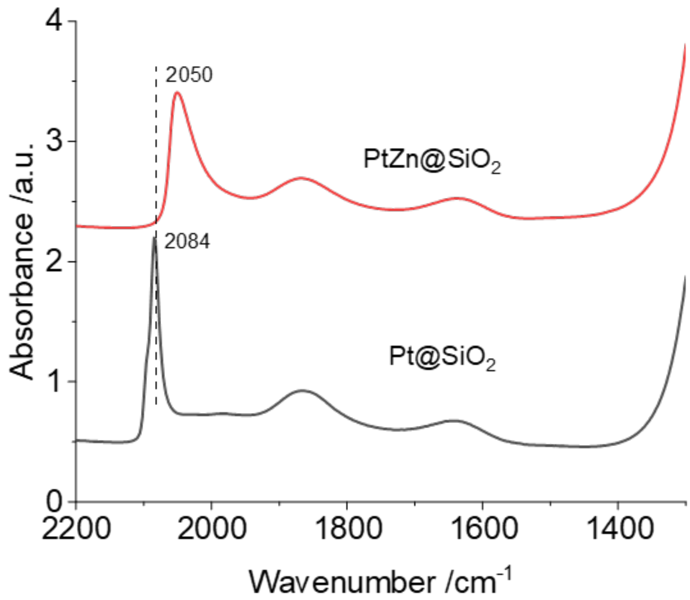

Figure S4. FIIR spectra of CO adsorbed on Pt@SiO_2 and PtZn@SiO_2 under 5 mbar of CO at room temperature.

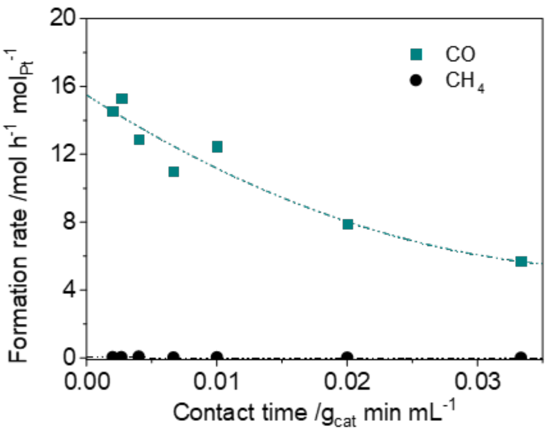

Figure S5. Product formation rates as a function of residence time over PtZn@SiO_2. Reaction conditions: $W_{cat.}$ = 200 mg, F = 6-100 mL/min, T = 230 ºC, P = 25 bar. Initial rates were extrapolated via a second order polynomial fit to the y axis.

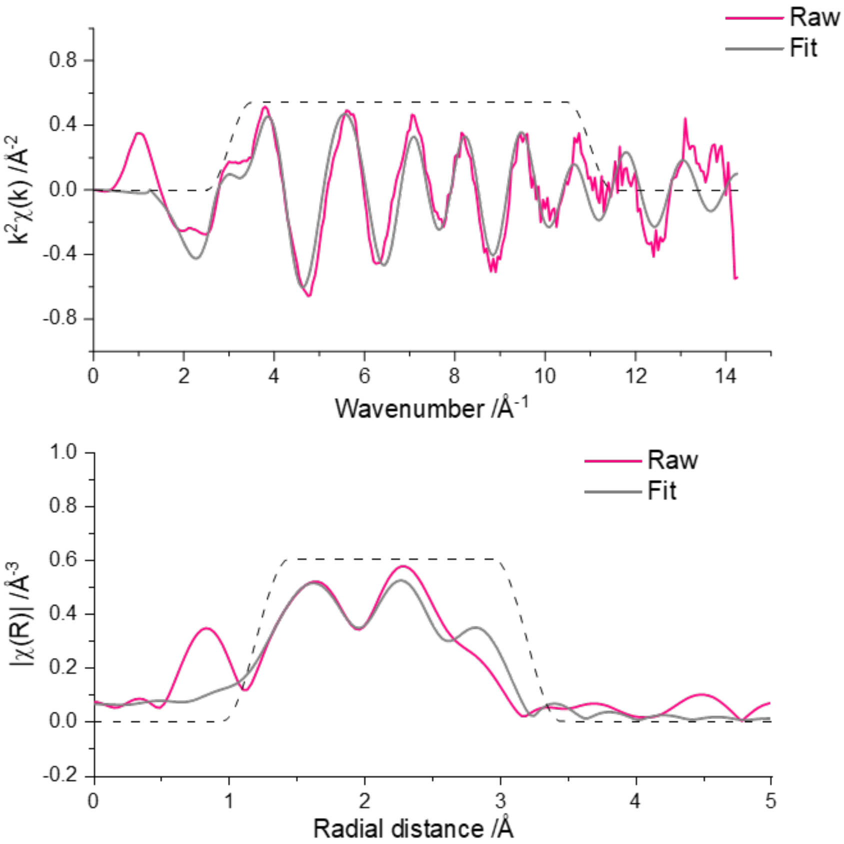

Figure S6. EXAFS fit for air exposed $PtZn@SiO_2$. (top) K-space with raw (pink) and fitted (gray) data. Window (black dotted line) 3.0-11 Å^{-1}, k-weight = 2, Hanning window, dk = 1; (bottom) R-space with raw (pink) and fitted (gray) data. Window (black dotted line) 1.2-3.2. Å, k-weight = 2, Hanning window, dk = 0.5. Fitting parameters are summarized in Table S2.

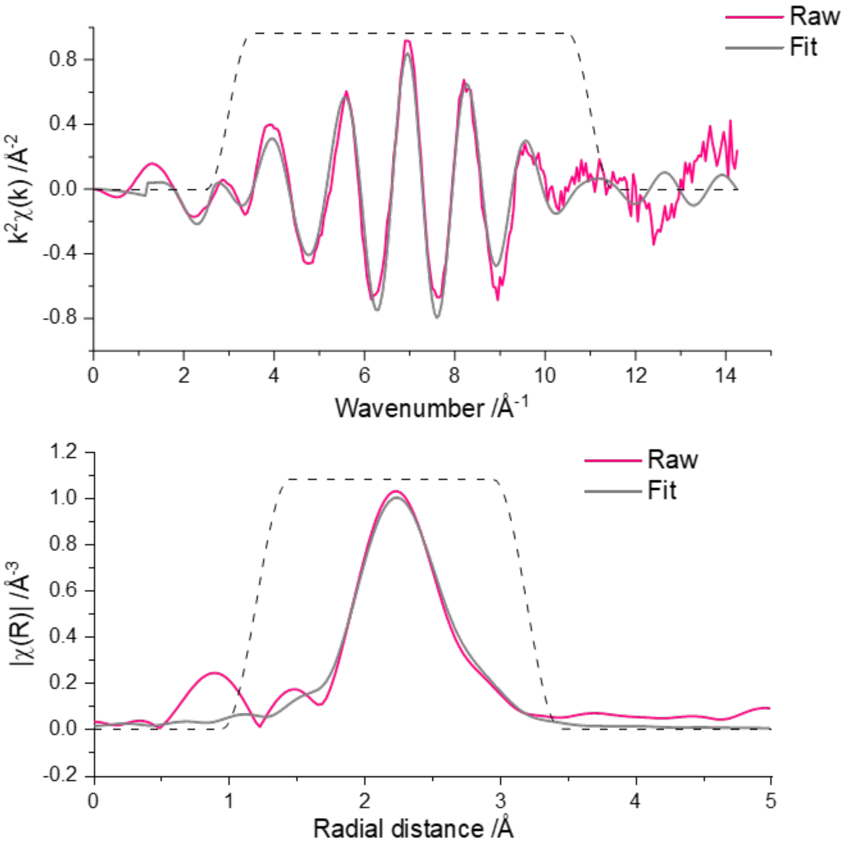

Figure S7. EXAFS fit for H_2 reduced PtZn@SiO_2. (top) K-space with raw (pink) and fitted (gray) data. Window (black dotted line) 3.0-11 Å^{-1}, k-weight = 2, Hanning window, dk = 1; (bottom) R-space with raw (pink) and fitted (gray) data. Window (black dotted line) 1.2-3.2. Å, k-weight = 2, Hanning window, dk = 0.5. Fitting parameters are summarized in Table S2.

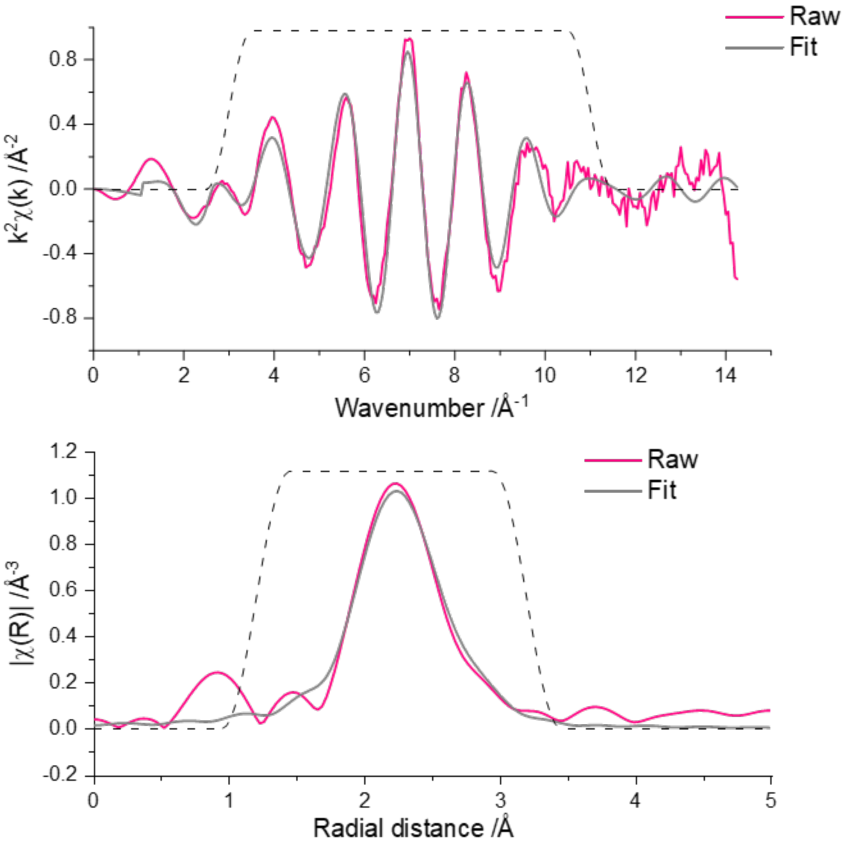

Figure S8. EXAFS fit for post CO_2 hydrogenation PtZn@SiO_2. (top) K-space with raw (pink) and fitted (gray) data. Window (black dotted line) 3.0-11 Å^{-1}, k-weight = 2, Hanning window, dk = 1; (bottom) R-space with raw (pink) and fitted (gray) data. Window (black dotted line) 1.2-3.2. Å, k-weight = 2, Hanning window, dk = 0.5. Fitting parameters are summarized in Table S2.

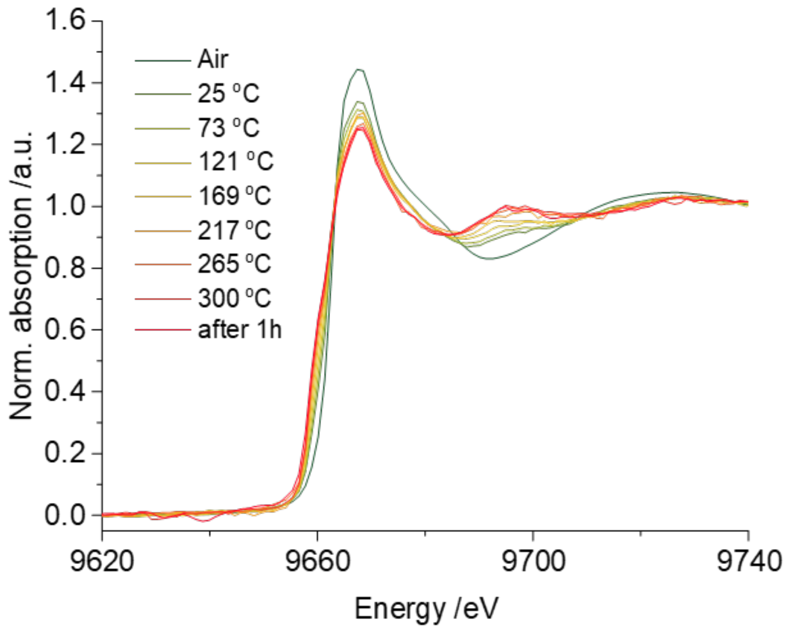

Figure S9. *In situ* Zn K-edge XANES spectra for $PtZn@SiO_2$ collected during H_2 temperature programmed reduction.

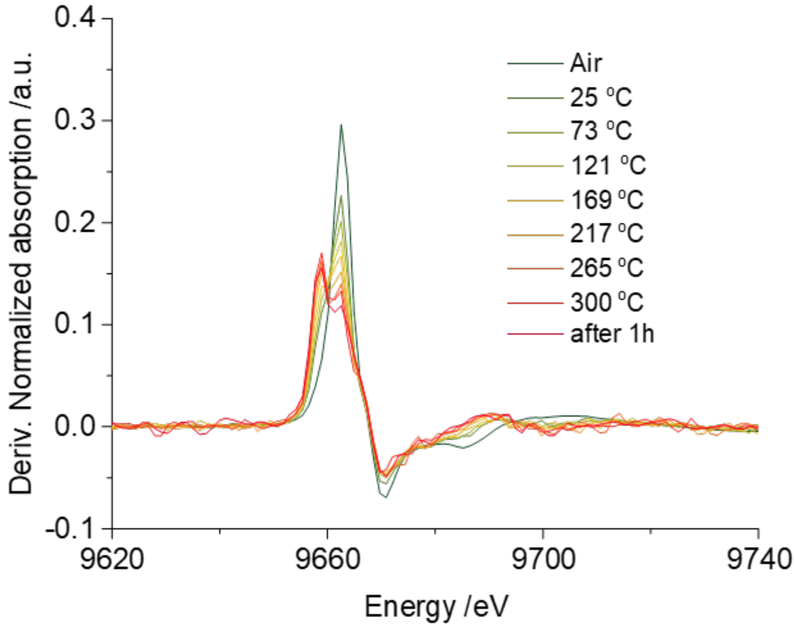

Figure S10. *In situ* Zn K-edge first derivate spectra for PtZn@SiO_2 collected during H_2 temperature programmed reduction.

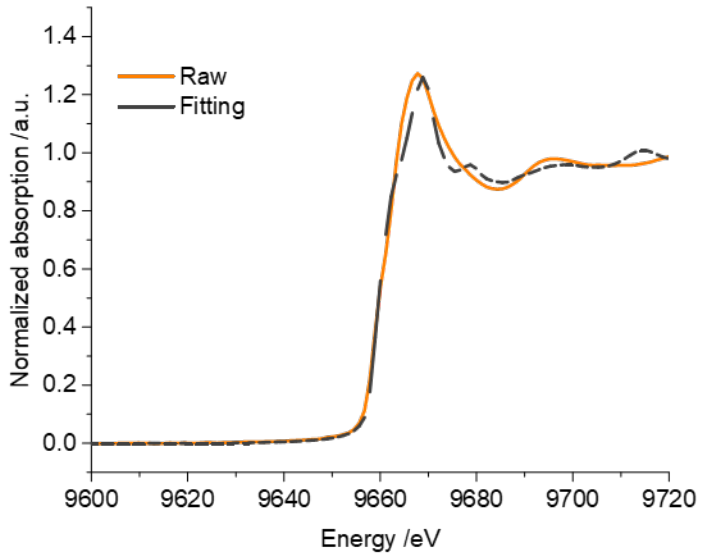

Figure S11. Linear combination fitting of Zn K-edge XANES for PtZn@SiO_2 after H_2 reduction. Zn^{II}@SiO_2 and Zn foil were used as references for the LCF.

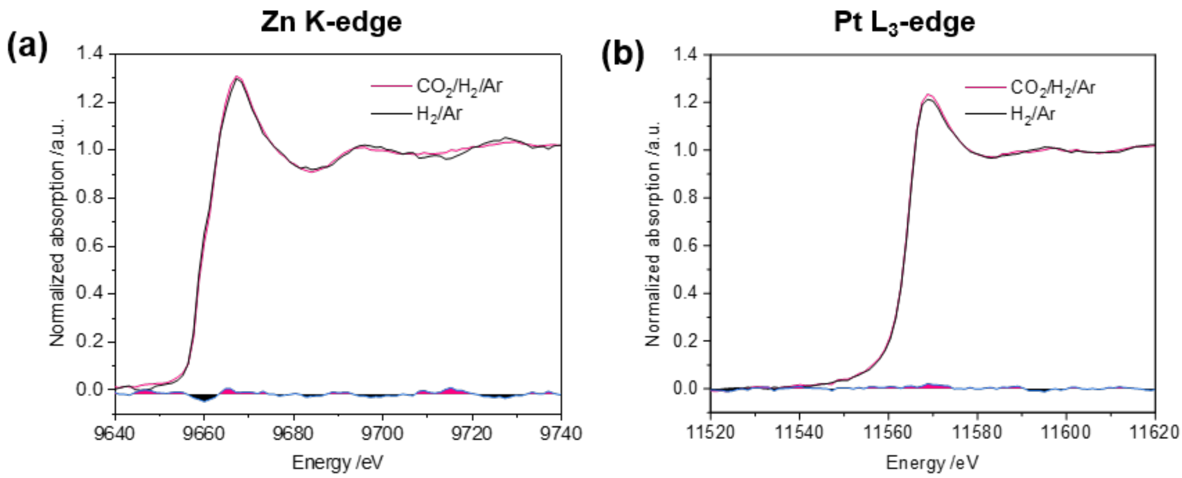

Figure S12. *In situ* XANES spectra of PtZn@SiO_2 collected under H_2/Ar (3:2, 20 bar) and under CO_2/H_2/Ar (1:3:1, 20 bar). (a) Zn K-edge spectra and (b) Pt L_3-edge spectra.

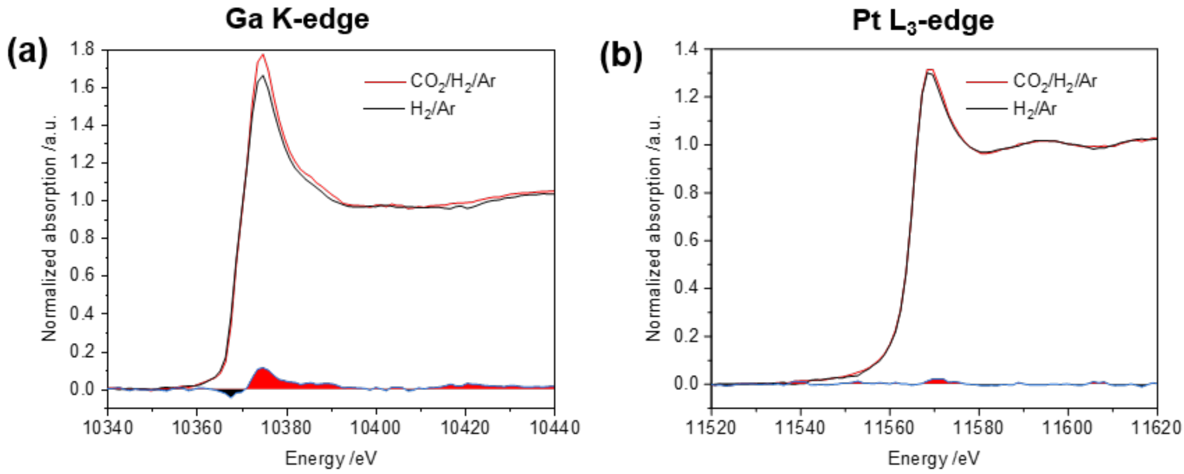

Figure S13. *In situ* XANES spectra of PtGa@SiO_2 collected under H_2/Ar (3:2, 20 bar) and under CO_2/H_2/Ar (1:3:1, 20 bar). (a) Ga K-edge spectra and (b) Pt L_3-edge spectra. The XAS results adapted from our previous work where identical conditions were used to collect the spectra. [1]

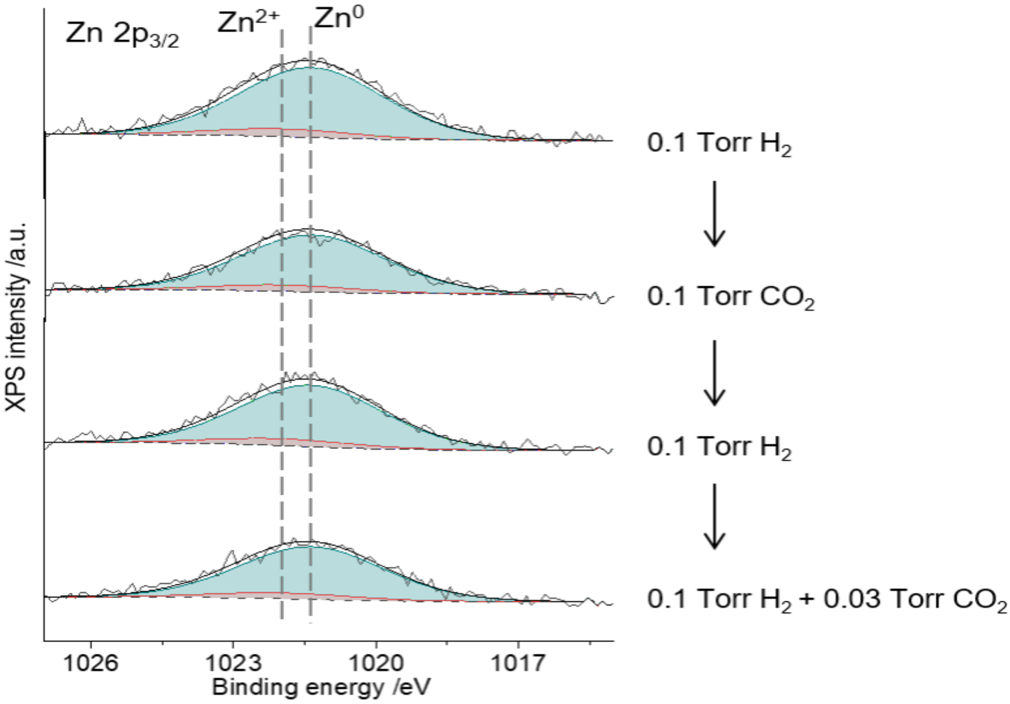

Figure S14. AP-XPS of Zn $2p_{3/2}$ spectra for PtZn@SiO_2.

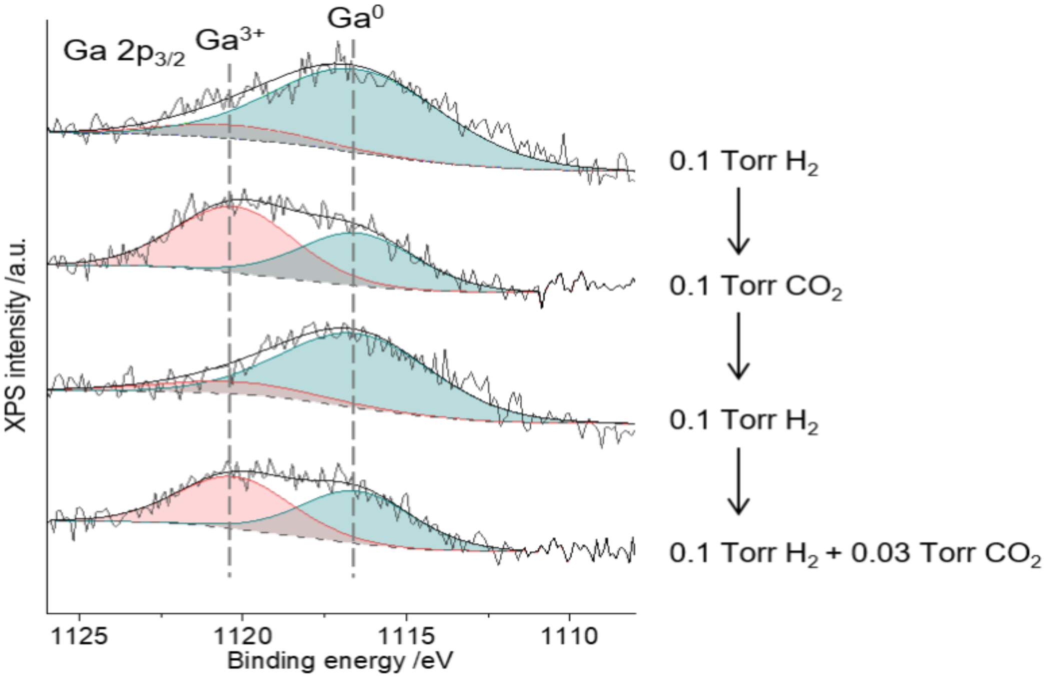

Figure S15. AP-XPS of Ga $2p_{3/2}$ spectra for PtGa@SiO_2.

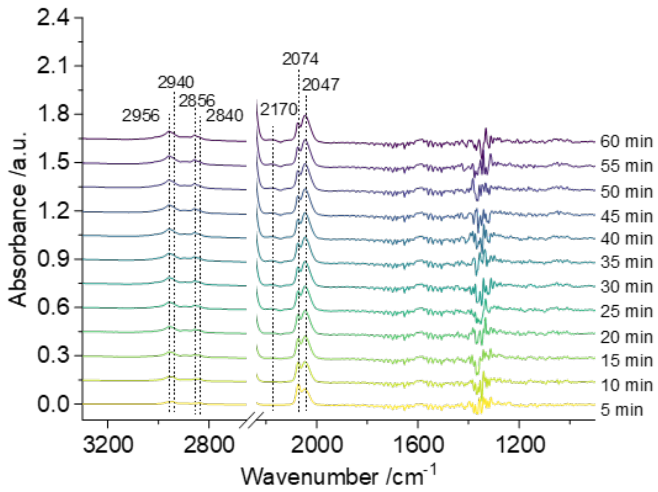

Figure S16. *In situ* DRIFTS for PtGa@SiO_2. The spectra were collected under $H_2/CO_2/Ar$ (3:1:1, 20 bar). The results adapted from our previous work where identical conditions were used to collect the spectra. [1]

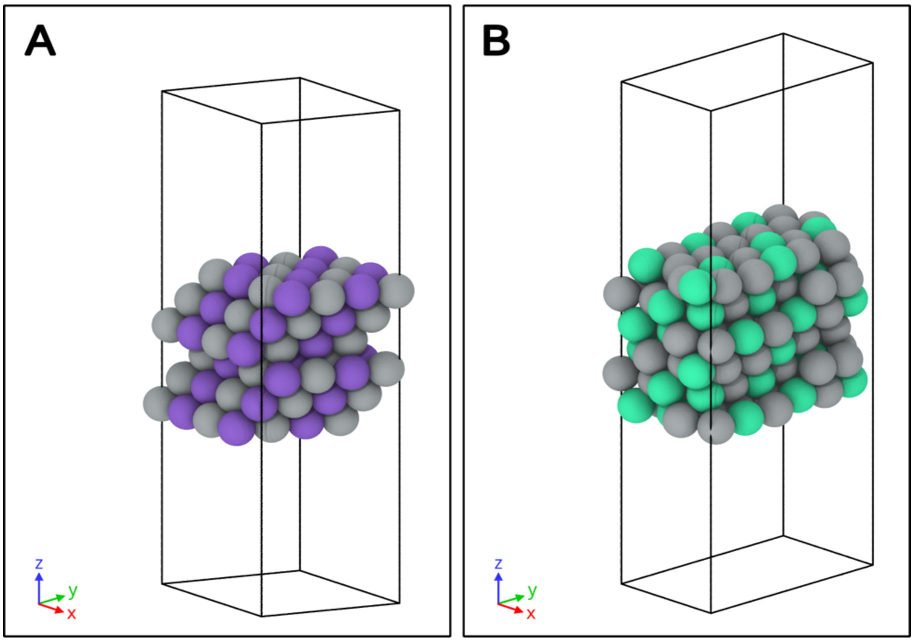

Figure S17. Unit cells of the slab models of PtZn(111) (panel A) and Pt2Ga(120) (panel B) used in the simulations.

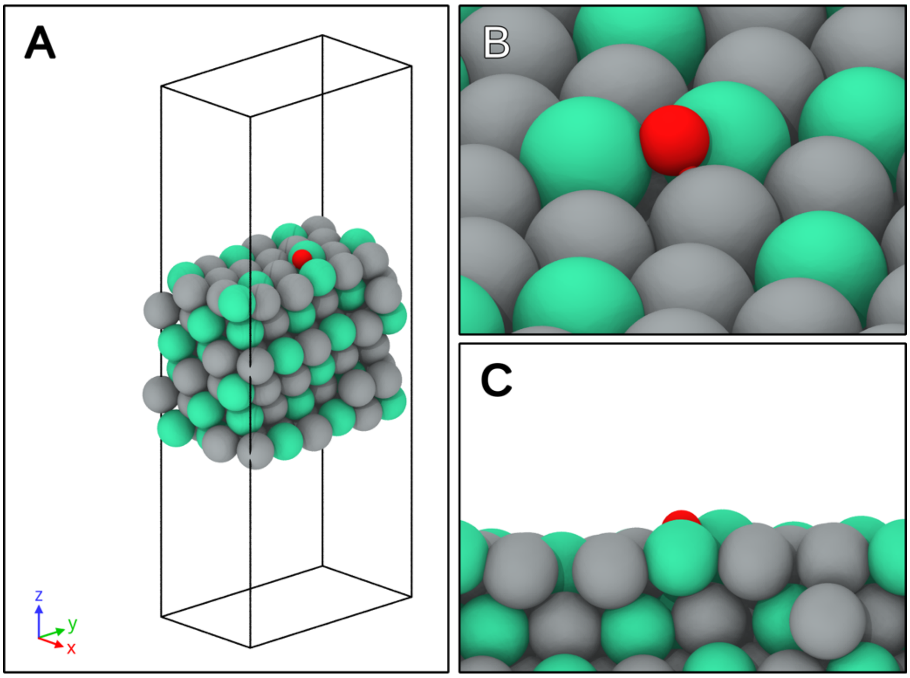

Figure S18. Simulation cell (panel A), detail of the adsorbate (panel B), and side view (panel C) of the pristine Pt2Ga(120) surface with one adsorbed oxygen atom.

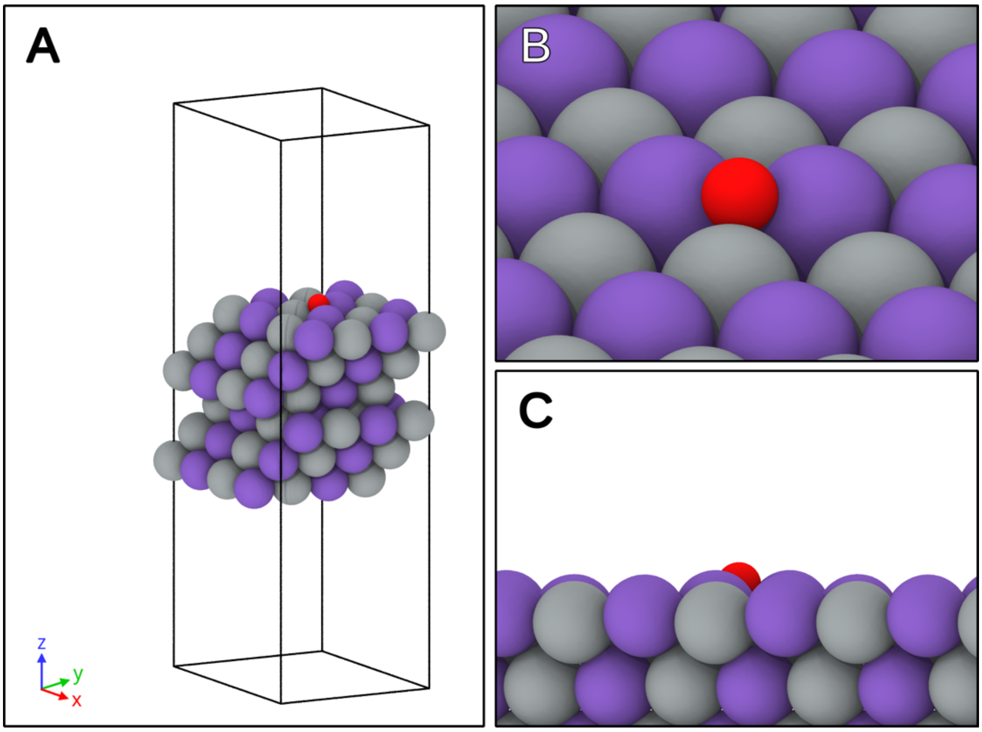

Figure S19. Simulation cell (panel A), detail of the adsorbate (panel B), and side view (panel C) of the pristine PtZn(111) surface with one adsorbed oxygen atom.

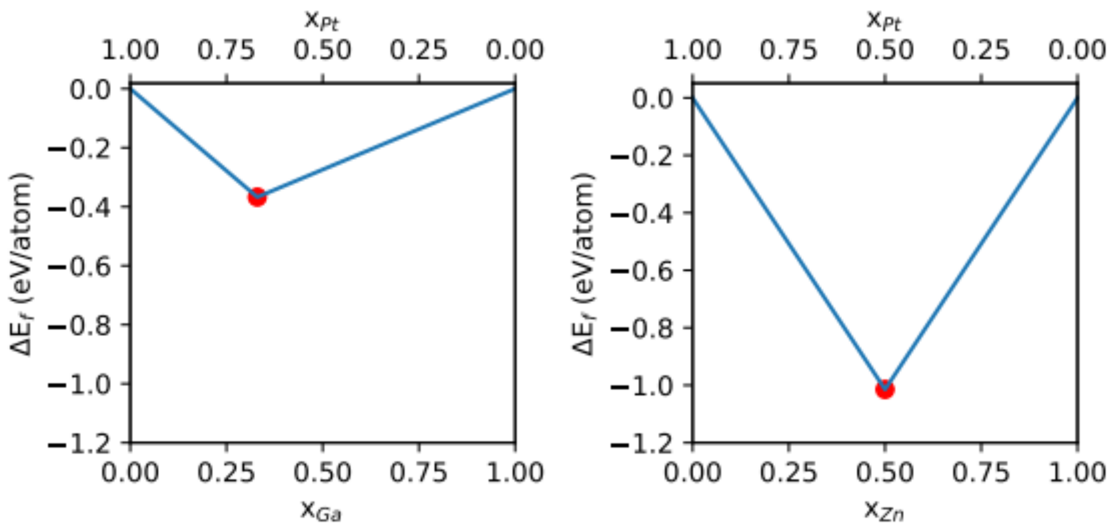

Figure S20. Mixing electronic energies (ΔE_f, in eV/atom) of bulk Pt_2Ga (left panel) and PtZn (right panel) with respect to the corresponding composing elements: Pt, Ga, and Pt, Zn, respectively.

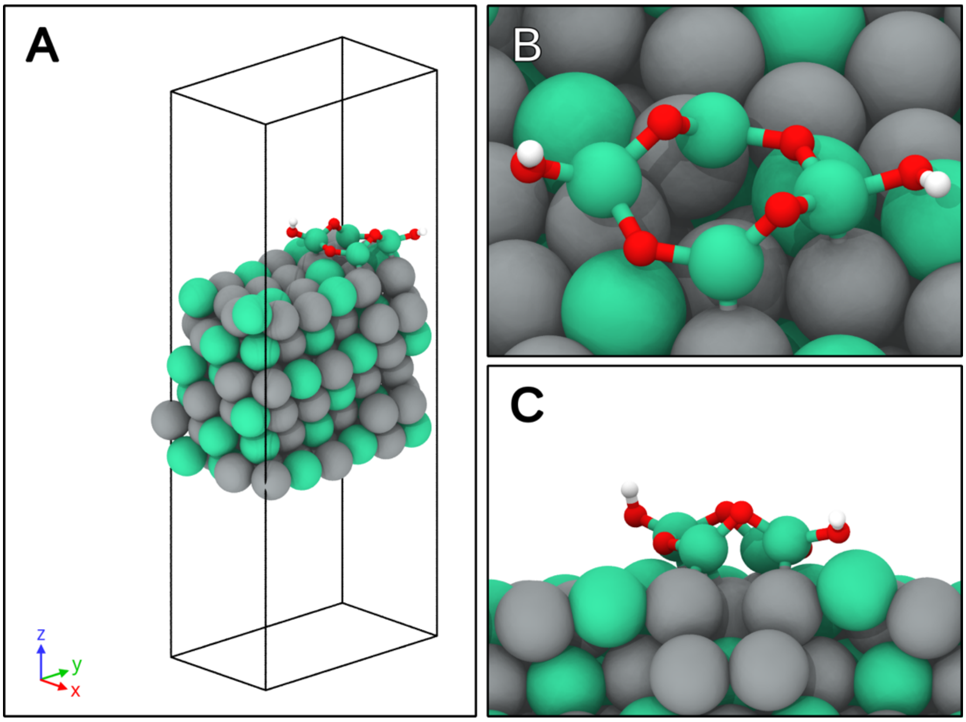

Figure S21. Simulation cell (panel A), detail of the active site (panel B), and side view (panel C) of the pristine Pt_2Ga-GaO_x surface.

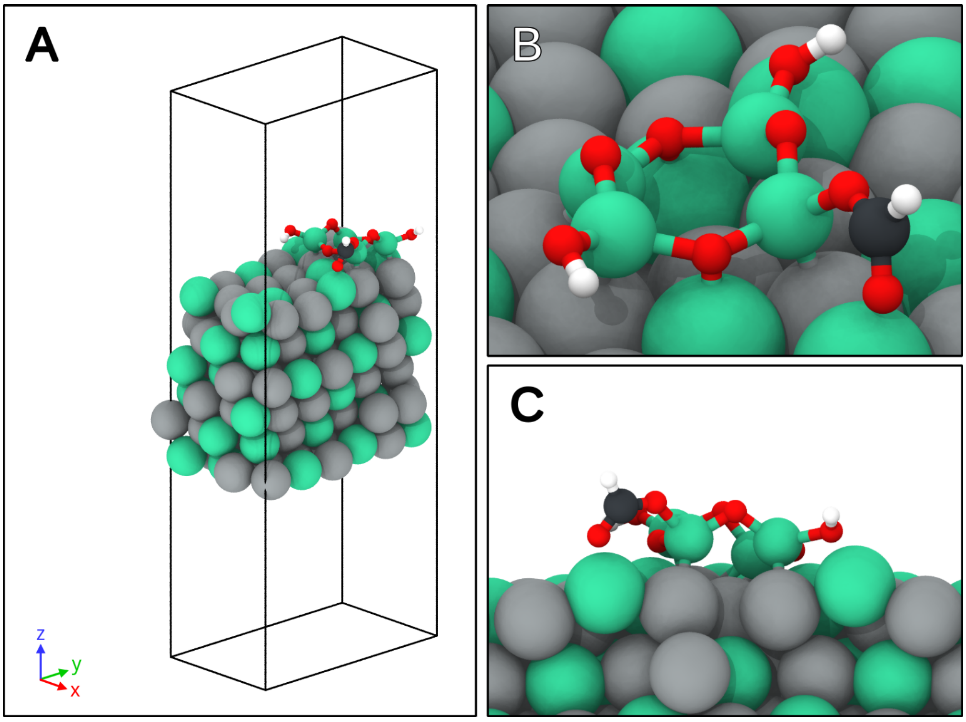

Figure S22. Simulation cell (panel A), detail of the adsorbate (panel B), and side view (panel C) of the pristine Pt_2Ga-GaO_x surface with adsorbed HCOO*.

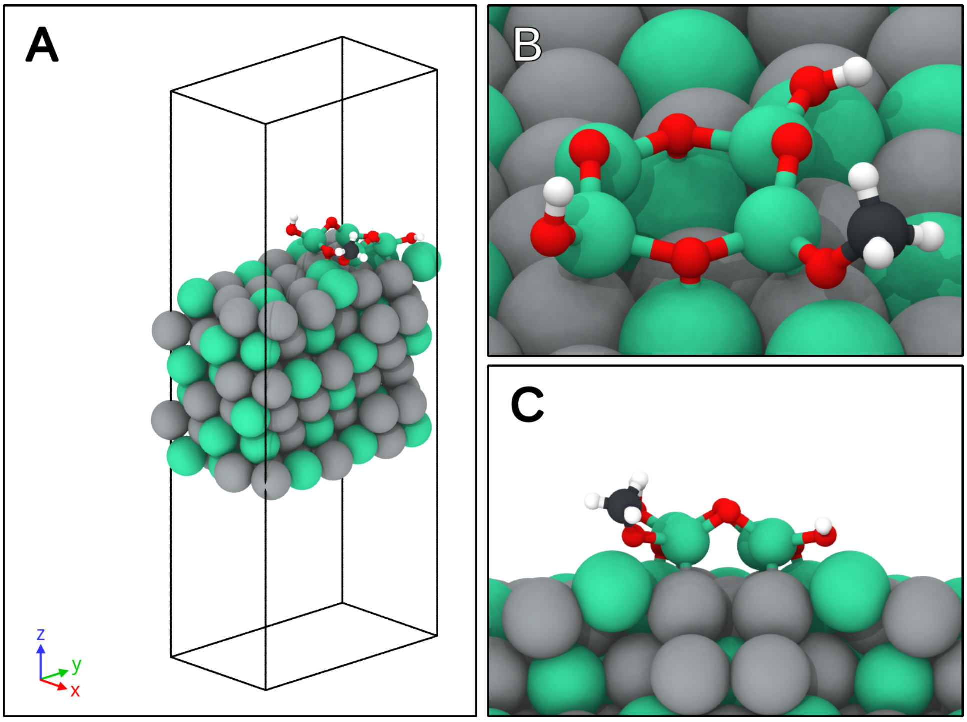

Figure S23. Simulation cell (panel A), detail of the adsorbate (panel B), and side view (panel C) of the pristine Pt_2Ga-GaO_x surface with adsorbed CH_3O^*.

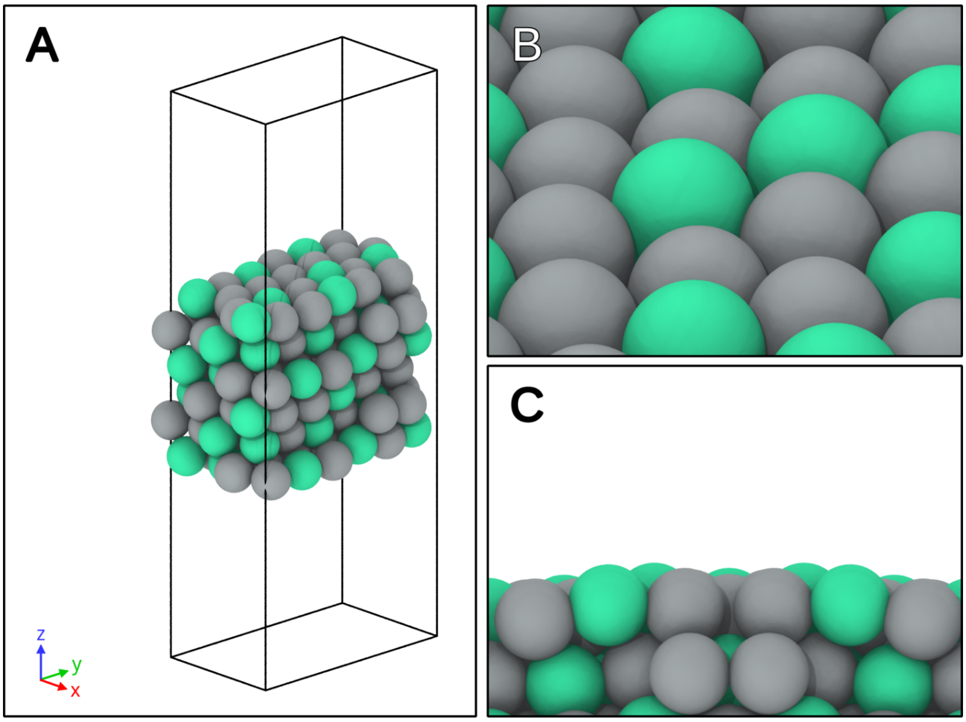

Figure S24. Simulation cell (panel A), detail of the surface (panel B), and side view (panel C) of the pristine $Pt_2Ga(120)$ surface.

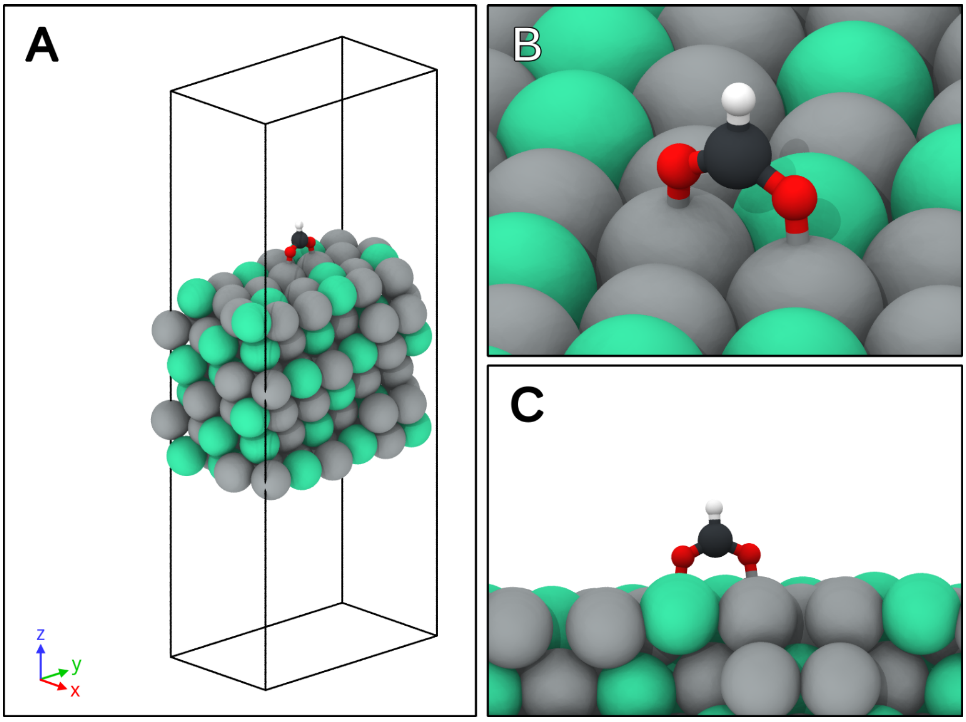

Figure S25. Simulation cell (panel A), detail of the adsorbate (panel B), and side view (panel C) of the $Pt_2Ga(120)$ surface with adsorbed HCOO*.

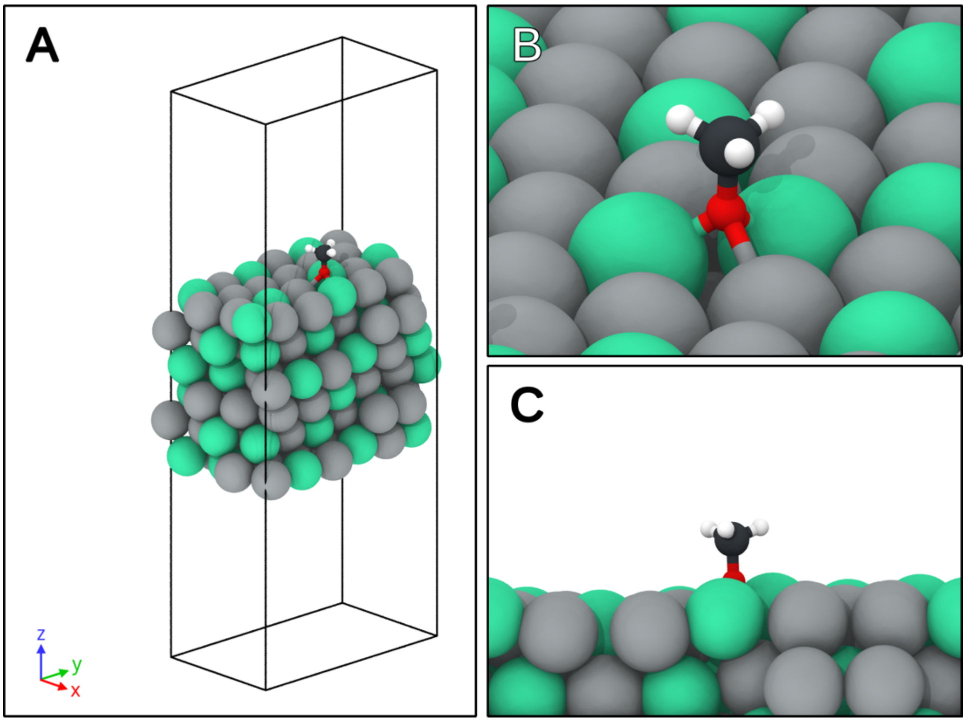

Figure S26. Simulation cell (panel A), detail of the adsorbate (panel B), and side view (panel C) of the $Pt_2Ga(120)$ surface with adsorbed CH_3O^*.

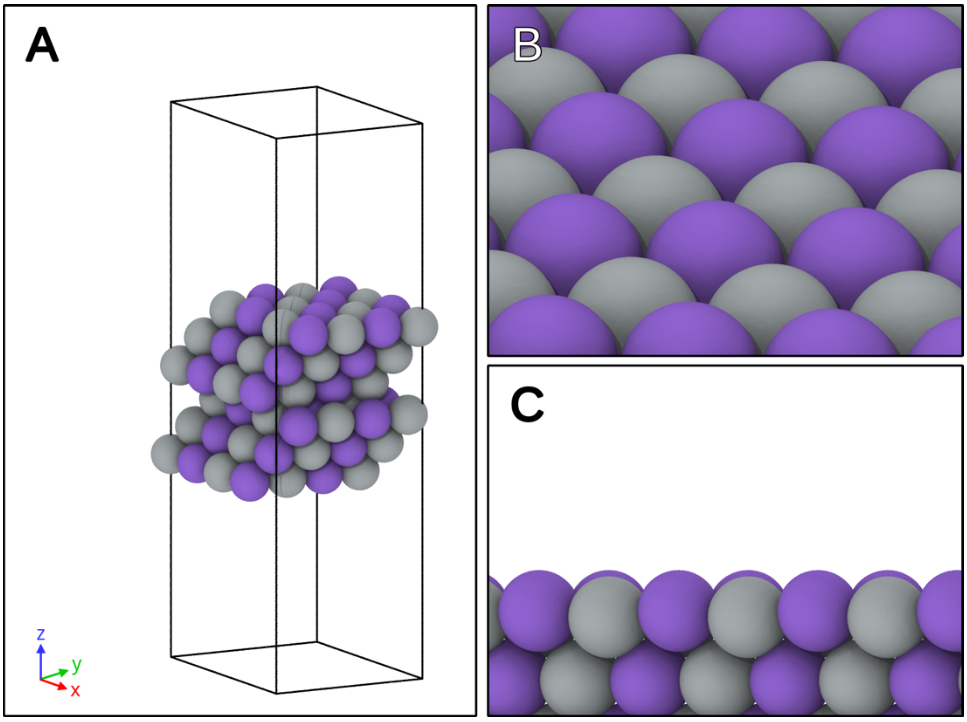

Figure S27. Simulation cell (panel A), detail of the surface (panel B) and side view (panel C) of the pristine PtZn(111) surface.

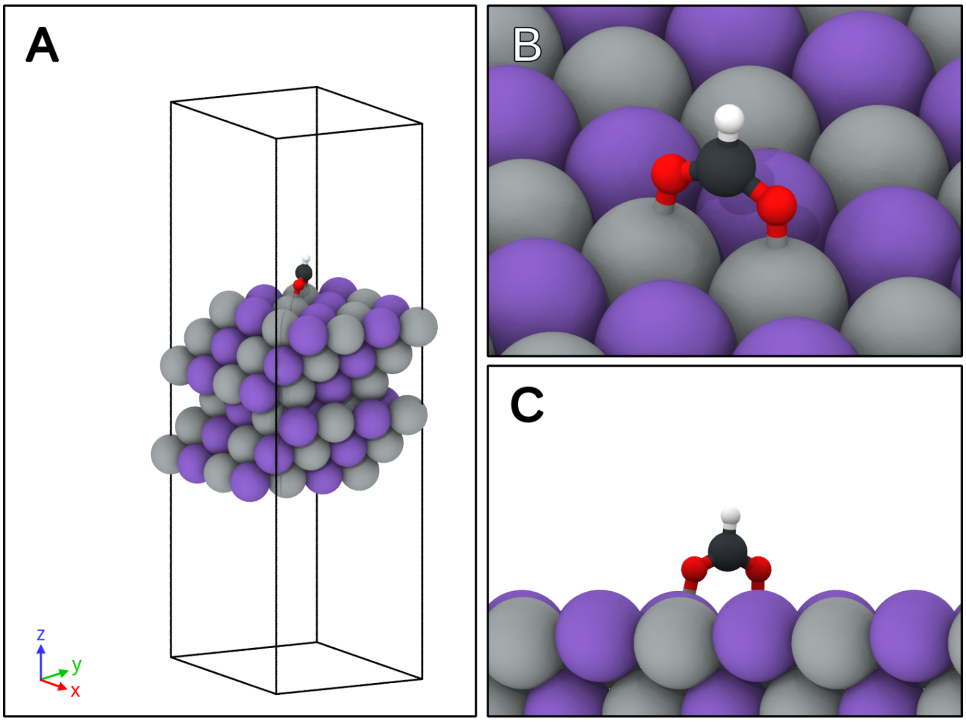

Figure S28. Simulation cell (panel A), detail of the adsorbate (panel B), and side view (panel C) of the PtZn(111) surface with adsorbed HCOO*.

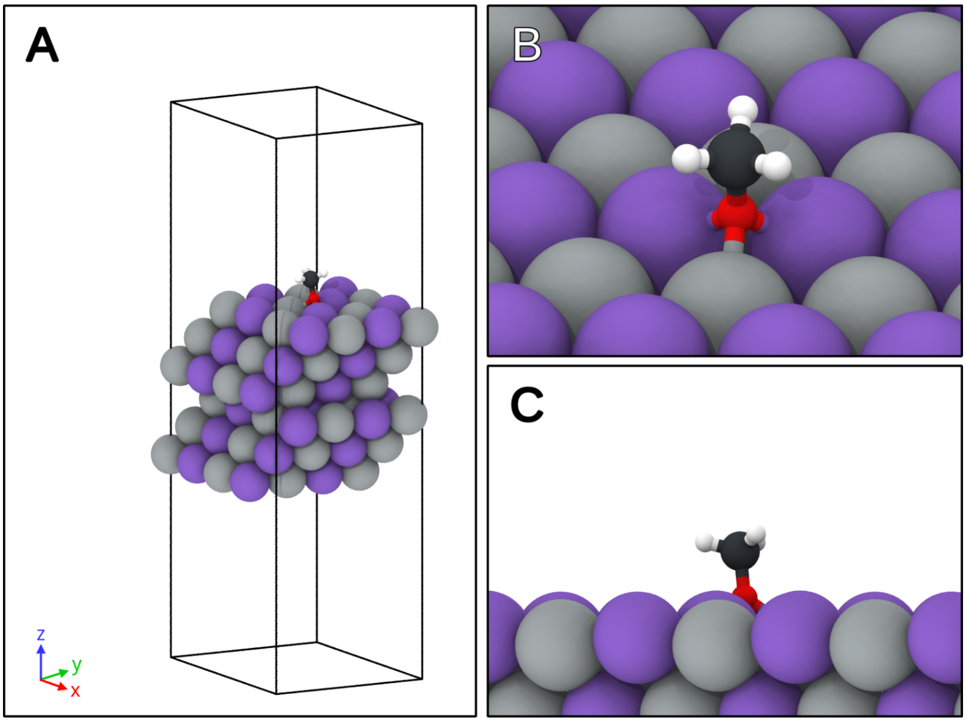

Figure S29. Simulation cell (panel A), detail of the adsorbate (panel B), and side view (panel C) of the PtZn(111) surface with adsorbed CH_3O*.

Table 1. Summary of physicochemical properties of Pt@SiO_2, PtGa@SiO_2 and PtZn@SiO_2.

Catalyst	Metal loading (wt%)[a]	Metal density (M nm^{-2})	Pt/*M* ratio[a]	Particle size (nm)[b]
Pt@SiO_2[c]	Pt: 4.18	Pt: 0.65	-	1.9 ± 0.6
PtGa@SiO_2 [c]	Pt: 4.53 Ga: 1.70	Pt: 0.70 Ga: 0.73	0.95:1	1.9 ± 0.8
PtZn@SiO_2	Pt: 4.40 Zn: 1.75	Pt: 0.68 Zn: 0.81	0.84:1	1.8 ± 0.7

[a] Determined by element analysis (EA); [b] Particle size determined by STEM. [c] adapted from our previous work

1

Table S2. Summary of intrinsic formation rate and selectivities of different catalysts for CO_2 hydrogenation. [a]

Catalyst	Intrinsic formation rate (mol h^{-1} mol_{TM}^{-1})			Intrinsic CH_4 Select. (%)	Intrinsic CO Select. (%)	Intrinsic CH_3OH Select. (%)
	CH_4	CO	CH_3OH			
Pt@SiO_2	0.87	1.73	0	33.5	66.5	0
PtZn@SiO_2	0.06	15.5	0	0.4	99.6	0
PtGa@SiO_2	0.09	6.14	7.24	0.7	45.6	53.7

[a] Reaction conditions: $W_{cat.}$ = 200 mg, F = 6-100 mL/min, T = 230 °C, P = 25 bar.

Table S3. Summary of Pt L_3-edge fitting results of PtZn@SiO_2 catalysts under different conditions.[a]

Catalyst	Conditions	Path	CN[b]	σ^2 (Å^2)[c]	ΔE (eV)[d]	R (Å)[e]
PtZn@SiO_2	Air	Pt-O	1.6(0.7)	0.0047(0.0008)	5.6 (2.8)	1.97(0.01)
		Pt-Pt	6.2(2.1)	0.0083(0.0026)	5.6 (2.8)	2.72(0.05)
	H_2 reduction	Pt-Zn	4.9(1.2)	0.0093(0.0019)	5.3 (1.9)	2.61(0.07)
		Pt-Pt	4.9(1.0)	0.0093(0.0019)	5.3 (1.9)	2.77(0.01)
	Post CO_2 hydro.	Pt-Zn	5.2(1.4)	0.0097(0.0022)	4.6 (2.2)	2.61(0.07)
		Pt-Pt	4.9(1.2)	0.0097(0.0022)	4.6 (2.2)	2.76(0.02)

[a] $3.0 < k < 11.0$; S_o^2 was fixed as 0.82 (from Pt foil); $1.2 < R < 3.2$; k-weight = 2. [b] coordination number. [c] Debye-Waller parameter. [d] energy correction factor. [e] interatomic distance.

Table S4. LCF results and composition of the alloyed PtZn nanoparticles for PtZn@SiO_2 catalysts after H_2 reduction.

Catalyst	**Element**	**Proportion (%)**	**Average Pt/Zn^0 ratio**
PtZn@SiO_2	Zn^{II}	20	1.05:1
	Zn^0	80	

Table S5. Adsorption energy of $HCOO^*$ and CH_3O^* species on different model surfaces.[a]

Model system	$E_{ads}(HCOO^*)$/eV	$E_{ads}(CH_3O^*)$/eV
PtZn	-3.00	-3.05
Pt_2Ga	-3.15	-2.97
$Pt_2Ga + GaO_x$	-3.61	-3.14

[a] E(Abs) = E(Slab + species) – E(slab) – E(species).

References:

1. Zhou, W.; Brack, E.; Ehinger, C.; Paterson, J.; Southouse, J.; Coperet, C. Reactivity Switch of Platinum with Gallium: From Reverse Water Gas Shift to Methanol Synthesis. *J. Am. Chem. Soc.* **2024,** *146*, 10806-10811.